

Transport properties of silver selenomolybdate glassy ionic conductors

B. Deb and A. Ghosh

Citation: *J. Appl. Phys.* **112**, 094110 (2012); doi: 10.1063/1.4764929

View online: <http://dx.doi.org/10.1063/1.4764929>

View Table of Contents: <http://jap.aip.org/resource/1/JAPIAU/v112/i9>

Published by the [American Institute of Physics](http://www.aip.org).

Related Articles

Electrical, dielectric and spectroscopic studies on MnO doped LiI–AgI–B₂O₃ glasses

J. Appl. Phys. **111**, 013714 (2012)

Inversion of the direction of photo-induced mass transport in As₂₀Se₈₀ films: Experiment and theory

J. Appl. Phys. **110**, 063502 (2011)

Proton conduction in hydrous glasses of the join CaAl₂Si₂O₈–CaMgSi₂O₆: An impedance and infrared spectroscopic study

J. Chem. Phys. **134**, 194505 (2011)

Dielectric and conductivity relaxation in AgI doped silver selenite superionic glasses

J. Appl. Phys. **108**, 074104 (2010)

Self-diffusion of poly(propylene glycol) in nanoporous glasses studied by pulsed field gradient NMR: A study of molecular dynamics and surface interactions

J. Chem. Phys. **133**, 094903 (2010)

Additional information on *J. Appl. Phys.*

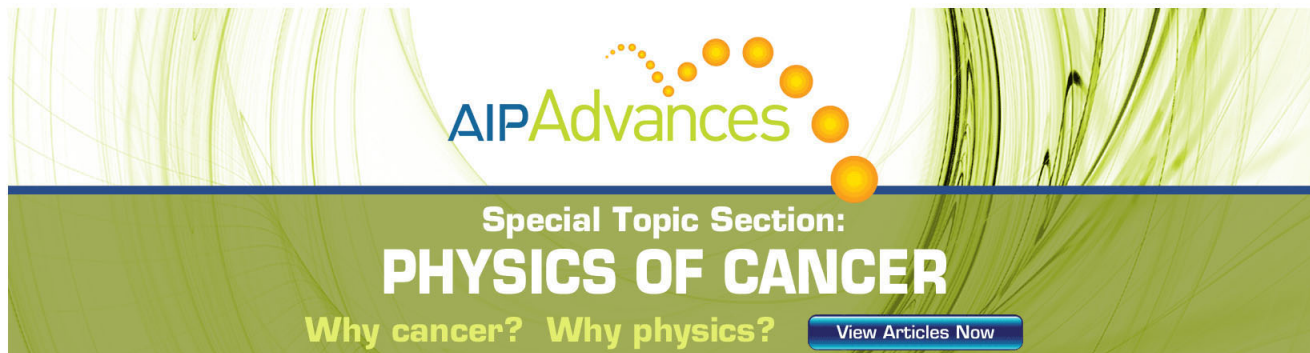
Journal Homepage: <http://jap.aip.org/>

Journal Information: http://jap.aip.org/about/about_the_journal

Top downloads: http://jap.aip.org/features/most_downloaded

Information for Authors: <http://jap.aip.org/authors>

ADVERTISEMENT



AIP Advances

Special Topic Section:
PHYSICS OF CANCER

Why cancer? Why physics? [View Articles Now](#)

Transport properties of silver selenomolybdate glassy ionic conductors

B. Deb^{a)} and A. Ghosh^{b)}

Department of Solid State Physics, Indian Association for the Cultivation of Science, Jadavpur, Kolkata 700032, India

(Received 20 August 2012; accepted 12 October 2012; published online 9 November 2012)

Transport properties of silver selenomolybdate glassy ionic conductors have been reported for wide composition and temperature ranges. It has been observed that the transport properties of these glasses depend strongly on the modifier content as well as on the glass formers ratio. A direct correlation between the ion transport and the modification of the glass structure has been predicted. Transport properties of these glasses are also strongly influenced by the existence of dual character of SeO_2 as a glass former and a glass modifier. Structural models for different compositions have also been proposed. © 2012 American Institute of Physics. [<http://dx.doi.org/10.1063/1.4764929>]

I. INTRODUCTION

The study of glassy ionic conductors is gaining significant attention in recent years for their uses in electrochemical devices.^{1,2} They are equally important from academic point of view to understand the ion transport properties in complex materials.³ The ion transport properties in glasses are mostly governed by the microscopic structural aspects of the glass network.⁴⁻⁶ The enhancement of conductivity in a systematic way is essentially the first criteria in selecting new ionic glass as a potential candidate. There are different ways in which the enhancement in conductivity can be achieved. The increase of modifier oxide (e.g., Ag_2O , Li_2O , etc.) preferentially breaks the glass network structure leading to depolymerization of the glass network and this in turn leads to the increase of non-bridging oxygen.⁷ In a few cases, addition of alkali halides causes an increase in the conductivity, which has been attributed to the expansion of the glass network,⁸ while in a few cases, addition of sulphide salts has been observed to increase the conductivity due to the increase in the polarizability of the glass.⁹ Another intriguing way to control the conductivity is to add different glass network formers,¹⁰ where the variation of conductivity depends on the glass formers ratio and the phenomenon is widely known as “mixed glass former effect” (MGFE).¹¹

In mixed former glasses such as borophosphate systems containing traditional glass formers, the variation of the ionic conductivity is correlated to a characteristic length scale determining the extent of correlated hopping motion of the ions obtained from the mean square displacement of ions.¹¹ These characteristic length scales show compositional dependence similar to that of tetrahedrally coordinated BO_4 units¹¹ indicating that the connectivity of the network forming units influences the conductivity. However, the study on conditional or non-traditional mixed glass former system is not extensive.¹² Recently, the study of few selenoborate glasses¹³ shows that with increasing SeO_2 content the formation of

Se-O cluster takes place in the glass network. These clusters in turn modify the boron-oxygen network and create more non-bridging oxygen. The increased mobility of cations is thus facilitated by increased polar cluster and highly depolymerized B-O network, as SeO_2 content increases.¹³ The variation of the macroscopic properties of mixed former glasses thus depends on the microscopic network forming units of these glasses. Recently, mixed barrier model¹⁴ has been proposed to explain the MGFE phenomenon. This model takes into account of the composition independent coordination environment of network forming units, and the strength of the barrier reduction due to mixing of two different glass formers has been estimated considering the reduction of jump barriers of the mobile ions in an environment consisting of different network units.

The understanding of ion conduction in glasses so far possesses a scientific challenge due to the complexity of the glass structure.¹⁵ Different theoretical models have been put forward to understand the conductivity and activation energy in different glasses.^{16,17} In a few cases, the variation of mobile ion concentration¹⁸ is considered to be a prominent factor influencing the ion transport, whereas in some other cases, the change of mobility¹⁹ caused by a change in glass structure is conceived to be the main factor governing the conductivity. The inherent problem thus lies in separating the contribution of mobility and mobile ion concentration to the total conductivity.¹⁵

In this paper, we report ion transport properties of selenomolybdate glassy ionic conductors for different modifier to glass former ratio. The dual role of SeO_2 as a glass modifier and as a glass former is predicted. A direct correlation between the macroscopic ion transport and the modification of glass network structure is established. This work thus shed some lights on the understanding of MGFE in glassy ionic conductors.

II. EXPERIMENTAL DETAILS

The glass systems of compositions $y\text{Ag}_2\text{O}-(1-y)(x\text{SeO}_2-(1-x)\text{MoO}_3)$ where $0.40 \leq x \leq 0.80$ for $y=0.20, 0.30,$ and 0.40 series were prepared using melt quenching technique. Appropriate amounts of AgNO_3 , SeO_2 , and MoO_3

^{a)}Present address: Department of Physics, Government Degree College, Dharmanagar, Tripura-799250, India.

^{b)}Author to whom correspondence should be addressed. Electronic mail: sspag@iacs.res.in.

were mixed and preheated in an alumina crucible at 400 °C for 2 h for denitrogenation of AgNO₃. The mixtures were then melted in the temperature range 550–650 °C depending on composition and equilibrated for 1 h. The melts were then rapidly quenched between two aluminum plates to obtain the glassy samples. Density of the samples was measured using Archimedes principle with acetone as immersion liquid. The structural changes in these glasses were explored using Fourier transform infrared (FTIR) spectra recorded in a FTIR spectrometer (PerkinElmer, model Spectrum100). The electrical measurements such as conductance and capacitance of these glasses were carried out using a LCR meter (QuadTech 7600) in the frequency range 10 Hz–2 MHz and in a wide temperature range.

III. RESULTS AND DISCUSSION

The dc conductivity (σ_{dc}) for the glass compositions has been calculated from the complex impedance plots. Fig. 1(a) shows the temperature dependence of the dc conductivity for selected compositions. It is noted that the dc conductivity follows the Arrhenius relation of the form

$$\sigma_{dc} = \sigma_0 \exp(-E_\sigma/k_B T), \quad (1)$$

where σ_0 is the pre-exponential factor, T is the absolute temperature, E_σ is the activation energy, and k_B is the Boltzmann constant. All other samples also show similar behavior. The values of activation energy E_σ have been calculated from the

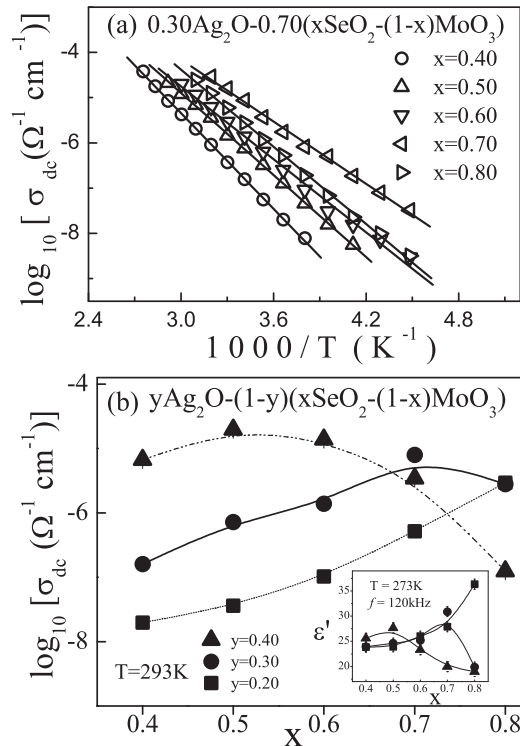


FIG. 1. (a) Variation of dc conductivity (σ_{dc}) as a function of reciprocal temperature for selected glasses of compositions $0.30\text{Ag}_2\text{O}-0.70(x\text{SeO}_2-(1-x)\text{MoO}_3)$. The solid lines are the least square linear fit to the data. (b) Compositional dependence of dc conductivity at 293 K for the glass compositions $y\text{Ag}_2\text{O}-(1-y)(x\text{SeO}_2-(1-x)\text{MoO}_3)$. The inset in (b) shows the compositional dependence of dielectric constant (ϵ') at a fixed frequency and temperature (shown). The lines are guide to the eye.

least squares straight line fits to the data and are listed in Table I. The variation of σ_{dc} as a function of SeO₂ content (x) at a fixed temperature (293 K) is shown in Fig. 1(b). It is observed that σ_{dc} for the $y=0.20$ series increases with increase of x, whereas σ_{dc} for the $y=0.30$ series increases up to $x=0.70$ and then decreases slightly for $x=0.80$. For $y=0.40$ series, σ_{dc} increases with increase of x up to 0.50 and then decreases for $x \geq 0.60$. The variation of activation energy shows an opposite trend to that of σ_{dc} for all the three series. From these results, it is noted that the conductivity depends strongly on the composition.

The composition dependence of the activation energy and the dc conductivity for the three series can be explained considering the Anderson-Stuart model.^{16,20} According to this model, the total activation energy (E_{AS}) comprises of two energy terms, namely, (a) electrostatic binding energy which is associated with the removal of the mobile cation from its bonded or occupied site and (b) the elastic strain energy associated with the creation of doorway for the mobile ion to pass or squeeze through. The total energy thus can be written in the form as follows:

$$E_{AS} = E_B + E_S. \quad (2)$$

Here, E_B and E_S are the binding energy and strain energy, respectively, given as

$$E_B = \frac{ZZ_0 e^2}{\gamma} \left(\frac{1}{r+r_0} - \frac{1}{R/2} \right), \quad (3a)$$

$$E_S = \frac{\pi}{2} G(r-r_d)^2 R, \quad (3b)$$

where γ is a covalence parameter related to the high frequency dielectric constant [$\epsilon'(\infty)$], Z and Z_0 are charges on the cation and oxide ions, respectively, with ionic radii r and r_0 , R is the ion-ion jump distance, and r_d is the doorway radius related to the opening or the creation of passage for mobile ions. The binding energy depends primarily on $\epsilon'(\infty)$, while the strain energy depends on the jump distance and doorway radius. Thus, the decrease of binding energy is related to the increase of dielectric constant, while the decrease of the strain energy is related to the increase of the doorway radius for the ion migration and consequently to the expansion of the local structure and on the decrease of jump distance. The dielectric property for the present samples was reported elsewhere.²¹ The composition dependence of ϵ' at a fixed frequency is shown in the inset of Fig. 1(b). It has been noted that the variation of dielectric constant (ϵ') depends on the modifier to glass former ratio for the three series. For the $y=0.20$ series, ϵ' increases continuously with increase of x, whereas for $y=0.30$ series, it increases up to $x=0.70$ and decreases for $x=0.80$. Similarly for $y=0.40$ series, ϵ' increases up to $x=0.50$ and then decreases for $x \geq 0.60$. From Eq. (3a), it is thus noted that this variation will in turn cause opposite variation in the binding energy term. Further, we have calculated the average ion-ion jump distance (R) from density and compositions of the glasses. Fig. 2(a) shows the composition dependence of jump distance. It is observed that jump distance decreases with

TABLE I. The value of dc conductivity (σ_{dc}), dc activation energy (E_{σ}), average mobile ion-ion separation (R), cross-over frequency ω_c , ac activation energy (E_c), and frequency exponent n for the glasses of composition $y\text{Ag}_2\text{O} - (1-y)(x\text{SeO}_2 - (1-x)\text{MoO}_3)$.

Composition	$\log [\sigma_{dc} (\Omega^{-1} \text{cm}^{-1})]$ at 293 K (± 0.05)	E_{σ} (eV) (± 0.02)	R (\AA) (± 0.02)	$\log [\omega_c (\text{rad s}^{-1})]$ at 293 K (± 0.05)	E_c (eV) (± 0.02)	n (± 0.02)
$y = 0.20$						
$x = 0.40$	-7.70	0.74	4.91	4.27	0.78	0.64
$x = 0.50$	-7.44	0.70	4.88	4.60	0.65	0.65
$x = 0.60$	-6.98	0.64	4.82	5.03	0.62	0.63
$x = 0.70$	-6.28	0.61	4.75	5.79	0.61	0.65
$x = 0.80$	-5.53	0.49	4.69	6.67	0.44	0.64
$y = 0.30$						
$x = 0.40$	-6.79	0.70	4.30	5.29	0.71	0.63
$x = 0.50$	-6.14	0.60	4.27	6.08	0.51	0.65
$x = 0.60$	-5.85	0.53	4.23	6.37	0.48	0.64
$x = 0.70$	-5.10	0.45	4.19	6.94	0.33	0.65
$x = 0.80$	-5.55	0.56	4.21	6.76	0.54	0.65
$y = 0.40$						
$x = 0.40$	-5.17	0.46	3.91	7.13	0.49	0.64
$x = 0.50$	-4.70	0.44	3.85	7.62	0.47	0.66
$x = 0.60$	-4.86	0.48	3.87	7.49	0.50	0.65
$x = 0.70$	-5.46	0.58	3.86	7.07	0.56	0.64
$x = 0.80$	-6.90	0.69	3.98	5.56	0.59	0.63

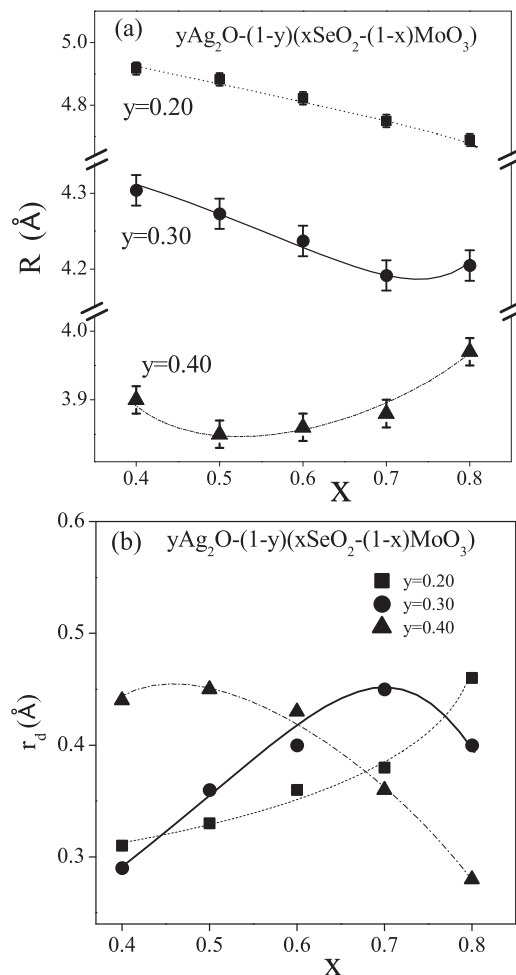


FIG. 2. (a) Compositional dependence of average mobile ion-ion jump distance, R , obtained from glass density and composition. (b) Doorway radius (r_d) obtained using Anderson-Stuart model. The lines are guide to the eye.

increase of x for $y = 0.20$ series, whereas for $y = 0.30$ series, it decreases up to $x = 0.70$ and increases for $x = 0.80$. For the $y = 0.40$ series, jump distance decreases up to $x = 0.50$ and then increases for $x \geq 0.60$. This variation leads to a proportional variation in the strain energy term. It is thus clearly noted that the combined effect is the effective variation in the binding energy and strain energy terms which together lead to the observed compositional dependence of the total activation energy. For calculating the strain energy, we have approximated the value of $G \sim 2 \times 10^{11}$ dyne/cm² as considered for other classes of oxide glasses reported.²⁰ Here, we consider the doorway radius to be composition dependent rather than constant, as we believe that the conductivity variation and modification of glass structure depending on glass former and modifier ratio is strongly related to the change in doorway radius. We quantify the total energy by adding binding energy and strain energy considering the doorway radius as a variable to get a close match to experimental activation energy. We thus obtain the composition dependence of doorway radius (r_d). The composition dependence of the doorway radius is shown in Fig. 2(b). It is clearly noted that r_d varies in a similar fashion as that of dc conductivity. For $y = 0.20$ series, the increase in doorway radius increases gradually which implies creation of more open network thus facilitating faster transport and thus increasing conductivity. For $y = 0.30$ series the doorway radius increases up to $x = 0.70$, and consequently, the conductivity also increases, whereas the doorway radius decreases slightly for $x = 0.80$ causing a drop in the conductivity. For $y = 0.40$ series, the increase continues up to $x = 0.50$ and then decreases for $x \geq 0.60$ causing the conductivity to vary in a similar fashion.

The ac conductivity ($\sigma(\omega)$) at several temperatures is shown in Fig. 3(a) for a glass composition as a function of frequency. At lower frequencies, the ac conductivity is almost independent of frequency corresponding to the dc

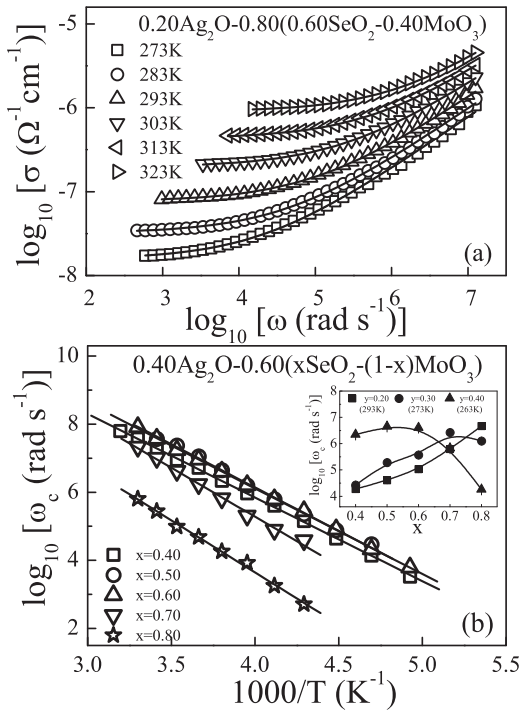


FIG. 3. (a) Ac conductivity spectra for the selected glass composition $0.20\text{Ag}_2\text{O}-0.80(0.60\text{SeO}_2-0.40\text{MoO}_3)$ at several temperatures are shown. The solid lines are fit to the power law. (b) The temperature dependence of crossover frequency, ω_c , for selected compositions $0.40\text{Ag}_2\text{O}-0.60(x\text{SeO}_2-(1-x)\text{MoO}_3)$. The solid lines are the linear fit to the data. Inset shows the compositional $y\text{Ag}_2\text{O}-(1-y)(x\text{SeO}_2-(1-x)\text{MoO}_3)$ at a fixed temperature (shown). The lines are guide to the eye.

conductivity. However, the ac conductivity shows dispersive behavior with the increase of frequency. The frequency dependence of the ac conductivity can be well described by a power law model¹⁵ given by

$$\sigma(\omega) = \sigma_{\text{dc}}[1 + (\omega/\omega_c)^n], \quad (4)$$

where n is a frequency exponent having value $0 < n \leq 1$ and ω_c is the crossover frequency signifying the transition from dc to dispersive region. The experimental data for different temperatures were fitted to Eq. (4), and the parameters σ_{dc} , ω_c and n were obtained from the fits. It was observed that the value of the dc conductivity obtained from the fits agreed well with those obtained from the complex impedance plots. The temperature dependence of ω_c for some selected composition is shown in Fig. 3(b), which indicates that the crossover frequency follows the Arrhenius relation with activation energy E_c similar to that of dc conductivity. The values of ω_c at a particular temperature for all the compositions are listed in Table I, and its composition dependence is shown in the inset of Fig. 3(b), which shows similar composition dependence as that of the dc conductivity. The values of E_c are obtained to be very close to E_σ indicating a common conduction mechanism.¹⁵ The value of frequency exponent n is almost independent of temperature and composition with an average value ~ 0.65 indicating a three dimensional conduction.²²

We show below that the ion transport in mixed network former glasses is associated with characteristic length scales.

The conductivity spectra can be expressed in terms of time-dependent mean square displacement, $\langle r^2(t) \rangle$, of the mobile ions in thermal equilibrium as follows:²³

$$\sigma'(\omega) = \frac{n_c q^2 \omega^2}{6k_B T H_R} \int_0^\infty \langle r^2(t) \rangle \sin(\omega t) dt, \quad (5)$$

where H_R is the Haven ratio, n_c is the mobile ion concentration, T is the absolute temperature, q is the elementary charge, and k_B is the Boltzmann constant. $\langle r^2(t) \rangle$ can be determined from the conductivity spectra via inverse transformation of Eq. (5),

$$\begin{aligned} \langle r^2(t) \rangle &= \frac{12k_B T H_R}{n_c q^2 \pi} \int_0^t dt' \int_0^\infty \frac{\sigma'(\omega)}{\omega} \sin(\omega t') d\omega, \\ &= \langle R^2(t) \rangle H_R, \end{aligned} \quad (6)$$

where $\langle R^2(t) \rangle$ is the displacement of the centre of charge of mobile ions related to mean square displacement via H_R . The Haven ratio varies for different glass systems depending on alkali modifier content. Since in our glass system values of H_R are unknown, we consider the effect of $\langle R^2(t) \rangle$ only.²⁴ Fig. 4(a) shows the scaled spectra of $\langle R^2(t) \rangle$ in time domain at several temperatures for a selected composition. It is noted that the spectra follow Summerfield scaling where the time scale is scaled by the product of the dc conductivity and the absolute temperature. It is observed that at long times,

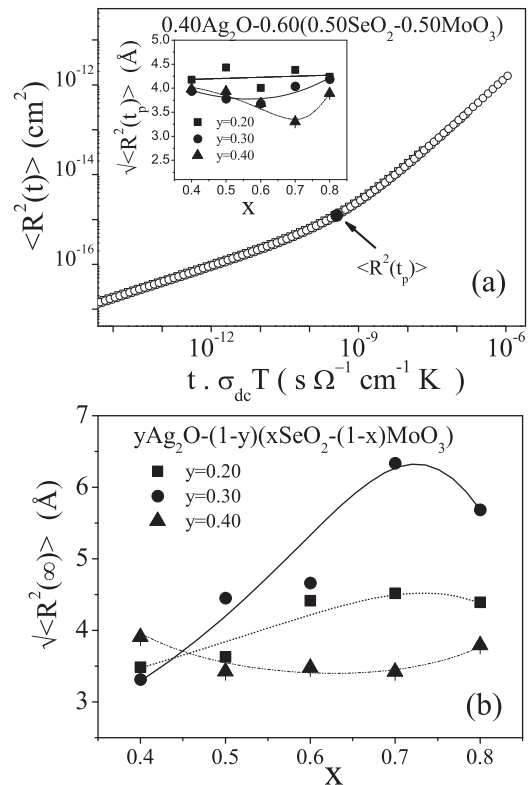


FIG. 4. (a) Scaled $\langle R^2(t) \rangle$ spectra following Summerfield scaling for a selected composition at several temperature are shown. Inset shows the composition dependence of characteristic length scale $\langle R^2(t_p) \rangle$ for the glass compositions $y\text{Ag}_2\text{O}-(1-y)(x\text{SeO}_2-(1-x)\text{MoO}_3)$. (b) The composition dependence of sub-diffusive length scale $\langle R^2(\infty) \rangle$. Lines are the guide to the eye.

$\langle R^2(t) \rangle$ reflects diffusive behavior, whereas at short times, the ion dynamics is of sub-diffusive. Following earlier report,²³ we define the characteristic transition time as t_p , which signifies the transition from sub-diffusive to diffusive behavior. At shorter time scale, the ion dynamics is thus characterized by correlated forward–backward hops, whereas at longer time scales, the ions can perform successful hops to the neighboring sites by crossing over the barriers or long range diffusion occurs. The characteristic length $\sqrt{\langle R^2(t_p) \rangle}$ would thus signify the distance the mobile ions have to travel in order to overcome the forces causing the correlated forward–backward motion. The value of $\sqrt{\langle R^2(t_p) \rangle}$ as obtained for the present mixed former glass systems depends on the modifier (y) as well as on the glass former contents (x) as shown in the inset of Fig. 4(a). For the $y=0.20$ series, $\sqrt{\langle R^2(t_p) \rangle}$ is almost constant (4.2 Å–4.3 Å) for all values of x . For the $y=0.30$ series, $\sqrt{\langle R^2(t_p) \rangle}$ initially decreases from 4.0 Å to 3.8 Å with the increase of x up to 0.70 and then increases up to 4.2 Å for $x=0.80$, whereas for the $y=0.40$ series, $\sqrt{\langle R^2(t_p) \rangle}$ decreases from 4.1 Å for $x=0.40$ to 3.3 Å for $x=0.50$ and then increases for $x \geq 0.60$ up to 3.9 Å for $x=0.80$. It is thus noted that for low modified glass ($y=0.20$), the length scale is almost independent of x . For intermediate ($y=0.30$) and highly modified ($y=0.40$) glasses, the length scale shows reverse correlation to that of the dc conductivity. This might be due to the dual role of SeO_2 as a modifier and a former, where it behaves as modifier for $y=0.20$ series and shows former like behavior as y increases from 0.30 to 0.40.

Another characteristic length scale, $\sqrt{\langle R^2(\infty) \rangle}$ can be defined, which signify the spatial extent of sub-diffusive motion of the mobile ion. This value can be deduced from the dielectric permittivity data using the following relation:^{23,24}

$$\langle R^2(\infty) \rangle = \frac{6k_B T \epsilon_0}{n_c q^2} [\epsilon'(0) - \epsilon'(\infty)], \quad (7)$$

where $\epsilon'(0)$ and $\epsilon'(\infty)$ are the low frequency and high frequency limits of dielectric constant and ϵ_0 is the permittivity of free space. The value of $\epsilon'(0)$ and $\epsilon'(\infty)$ is determined from the frequency dependence of real part ($\epsilon'(\omega)$) of complex permittivity $\epsilon^*(\omega) = \epsilon'(\omega) - i\epsilon''(\omega)$.²¹ Fig. 4(b) shows the compositional dependency of $\sqrt{\langle R^2(\infty) \rangle}$. For the $y=0.20$ series, $\sqrt{\langle R^2(\infty) \rangle}$ increases slightly with increase of x from 3.5 Å to 4.3 Å and then is almost independent of x . For the $y=0.30$ series, $\sqrt{\langle R^2(\infty) \rangle}$ increases with increase of x from 3.3 Å for $x=0.40$ to 6.0 Å for $x=0.70$ and then decreases to 5.7 Å for $x=0.80$ varying in a similar fashion to that of dc conductivity. For the $y=0.40$ series, $\sqrt{\langle R^2(\infty) \rangle}$ initially decreases from 4.0 Å for $x=0.40$ to 3.4 Å for $x=0.50$ and then increases for $x \geq 0.60$ up to 3.9 Å for $x=0.80$. It is thus noted that for low and intermediate modified glasses, $\sqrt{\langle R^2(\infty) \rangle}$ varies in a similar fashion to that of the dc conductivity. For strongly modified glasses, the variation of $\sqrt{\langle R^2(\infty) \rangle}$ is in a reverse trend to that of the macroscopic transport properties.

It is noted that the compositional dependence of $\sqrt{\langle R^2(\infty) \rangle}$ and $\sqrt{\langle R^2(t_p) \rangle}$ is quite similar for the $y=0.20$ series. But, for the $y=0.30$ and 0.40 series, the behavior is quite

different and the two length scales behave differently. In our case, the value of $\sqrt{\langle R^2(\infty) \rangle}$ is slightly different from that of $\sqrt{\langle R^2(t_p) \rangle}$ similar to the case of sodium borate glasses.¹¹ In case of single network former glasses like sodium germanates, sodium borates, sodium silicate glasses, the values of $\sqrt{\langle R^2(\infty) \rangle}$ and $\sqrt{\langle R^2(t_p) \rangle}$ show similar compositional dependency. However, as recently reported for some AgI doped silver phosphate glasses,²⁴ a distinct difference in the behavior of $\sqrt{\langle R^2(\infty) \rangle}$ and $\sqrt{\langle R^2(t_p) \rangle}$ is observed. In the present glasses, the difference in the behavior of the two length scales might be due to the transition from modifier like behavior to former like behavior of SeO_2 glass former with changing composition. These facts indicate that the microscopic parameter depends strongly on the nature of network formers, composition, and the extent of structural modification.

We have estimated the concentration of mobile Ag^+ ions using the Nernst-Einstein relation given by

$$\sigma_{dc} = q^2 d^2 n_c \omega_H / 12\pi k_B T, \quad (8)$$

where n_c is the mobile ion concentration, q is the charge, d is the average jump distance which we have approximated as ion-ion distance R , and ω_H is the hopping frequency of charge carriers. Here, we have approximated the hopping frequency in Eq. (8) to the crossover frequency in Eq. (4). It has been discussed¹⁵ that the mobile ion concentration calculated using Almost West approximation and Nernst-Einstein relation is not exact for higher frequency (above few MHz) where the fits deviate to a greater extent and the actual mobile ion concentration could be lower than that estimated using Eq. (8). This is mainly because the mobile ion concentration depends on the consideration of the time scale. The data for our samples fit reasonably well to Eq. (8) and the obtained concentration of mobile Ag^+ ions is plotted as a function of temperature in Fig. 5(a) for selected compositions. It is noted that mobile ion concentration is almost independent of temperature. The composition dependence of n_c at a fixed temperature is shown in Fig. 5(b). It is clearly noted that n_c depends slightly on composition, and the variation depends on modifier to glass former ratio. It is noted that for the $y=0.20$ series, n_c is almost constant, whereas for the $y=0.30$ series, n_c initially increases up to $x=0.70$ and then decreases for $x=0.80$ and n_c decreases for $x \geq 0.60$ for the $y=0.40$ series. This variation of n_c influences the conductivity variation for glasses containing higher SeO_2 and Ag_2O contents.

To further quantify the microscopic origin of the conductivity dependence on composition and its possible relation with the microscopic glass structure, the FTIR spectra for all the glass samples were considered.²¹ From FTIR study, it was observed that the significant contributions to the structural modification with changing composition are from the absorption bands around $\sim 600 \text{ cm}^{-1}$ and $\sim 860 \text{ cm}^{-1}$. The variation of relative area under these two bands is shown in Fig. 6(a). For the $y=0.20$, the area corresponding to band around 860 cm^{-1} changes negligibly up to $x=0.70$ and increases for $x=0.80$, while for the $y=0.30$ series, the area increases up to $x=0.70$ and decreases slightly for $x=0.80$. For the $y=0.40$ series, area of this band increases up to

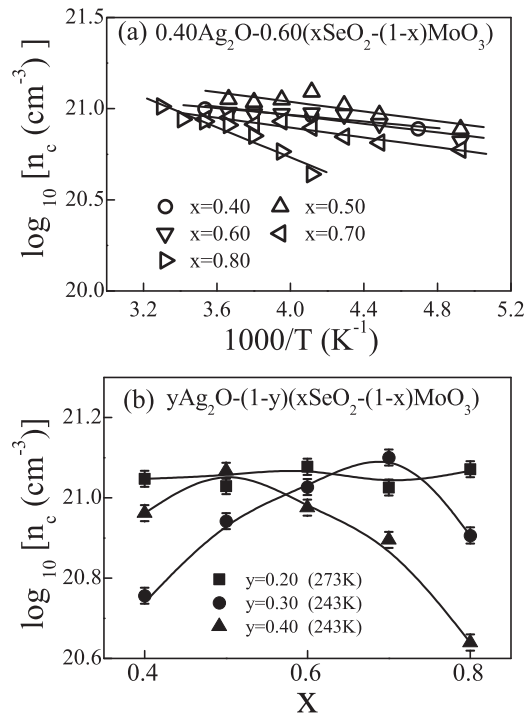


FIG. 5. Temperature dependence of mobile ion concentration, n_c , for selected glasses of compositions $0.40\text{Ag}_2\text{O}-0.60(x\text{SeO}_2-(1-x)\text{MoO}_3)$. (b) Compositional dependence of n_c at a fixed temperature (shown) for the glasses of compositions $y\text{Ag}_2\text{O}-(1-y)(x\text{SeO}_2-(1-x)\text{MoO}_3)$. The solid lines are guide to the eye.

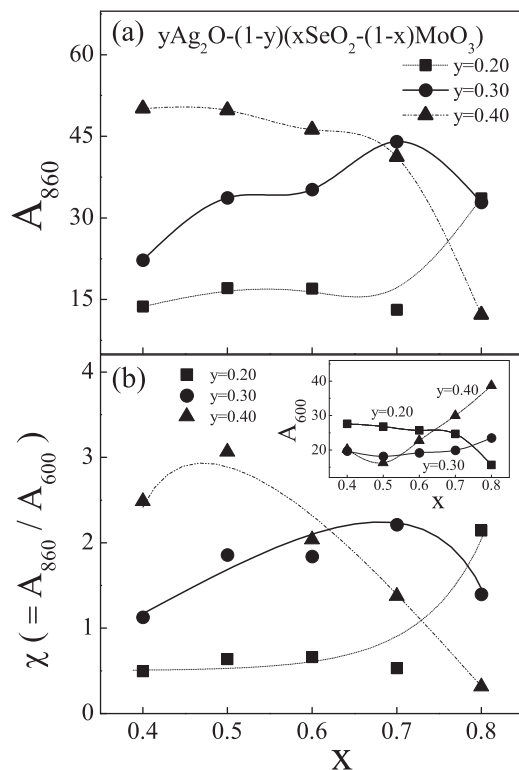


FIG. 6. Compositional variation of the relative band proportion for the absorption band at (a) $\sim 860\text{cm}^{-1}$ (A_{860}). (b) The composition dependence of the ratio of band proportion of A_{860} and A_{600} denoted as $\chi (=A_{860}/A_{600})$. The inset shows the proportions of the absorption band $\sim 600\text{cm}^{-1}$ (A_{600}) for the glass compositions $y\text{Ag}_2\text{O}-(1-y)(x\text{SeO}_2-(1-x)\text{MoO}_3)$. The lines are guide to the eye.

$x=0.50$ and then decreases for $x \geq 0.60$. The area of the absorption band around 600cm^{-1} decreases slightly with increase of x for the $y=0.20$ series, whereas for $y=0.30$ series, there is a slight increasing behavior for higher x . For the $y=0.40$ series, the area of absorption band around 600cm^{-1} first decreases up to $x=0.50$ and then increases for $x \geq 0.60$. So, at high modifier and high SeO_2 content, a decrease in the vibration mode of 860cm^{-1} and an increase of vibration mode at 600cm^{-1} are observed. The modification of glass network structure thus depends on glass formers ratio as well as on modifier content. The correlation to the conductivity thus can be drawn by calculating the ratio of the area under the absorption bands around 860cm^{-1} and 600cm^{-1} (henceforth will be denoted as χ) as shown in Fig. 6(b). It is clearly noted that the variation of this ratio χ is similar to that of the dc conductivity, signifying that, indeed, a direct correlation between the modifications of the microscopic glass structure and the macroscopic ion dynamics exists. Thus, for lower SeO_2 content for the $y=0.20$ and 0.30 series, the vibration of SeO_3^{2-} ion being predominant, the polarizability and also the number of non-bridging hopping sites available for the mobile ion increase signifying the modifier role of SeO_2 which facilitates faster conduction and thus higher mobility and conductivity. But, for higher SeO_2 content ($x \geq 0.60$) for highly modified glasses ($y=0.40$ series), the vibration of isolated SeO_3^{2-} ions tends to decrease due to increased tendency of bonding of Ag^+ ions with SeO_3^{2-} ions leading to the formation of Ag_2SeO_3 crystalline structure, and this in turn also enhances the vibration of isolated MoO_6 units. For these compositions, SeO_2 behaves as glass former and this in turn reduces the availability of effective non-bridging hopping sites thereby reducing the mobility and thus the conductivity.

From the results obtained from FTIR data and the conductivity study, a schematic structure and modification of the glassy network with changing compositions have been proposed. We have here shown a purely schematic 2D representation of possible modification of the glass structure with changing compositions. In Figs. 7(a) and 7(b), we have shown the glass structure for $x=0.40$ and 0.80 for the $y=0.20$ series, respectively. In these compositions, the glass structure is essentially modified due to the increase of free passage and non-bridging hopping sites. Thus, the structure of glass for $x=0.40$ for $y=0.20$ series initially represented by Fig. 7(a) transforms to that shown in Fig. 7(b) due to increased free volume and thus enhanced mobility. So, for this series, the increase in mobility mainly enhances the conductivity. In Figs. 7(c)–7(e), we have shown the glass structure for the $y=0.30$ as well as for $y=0.40$ series. Here, the structure is controlled by a change in the mobility as well as a change in the mobile ion concentration. Fig. 7(c) represents the glass structure for $x=0.40$, $y=0.40$ composition. Fig. 7(d) represents the structure for $0.50 \leq x \leq 0.70$ compositions for the $y=0.30$ series, where the available free volume increases slightly and also the mobile ion concentration increases as x increases, which increases the conductivity. Fig. 7(d) also represents the structure for the $y=0.40$, $x=0.50$ composition where there is an increase in available free volume for conduction and

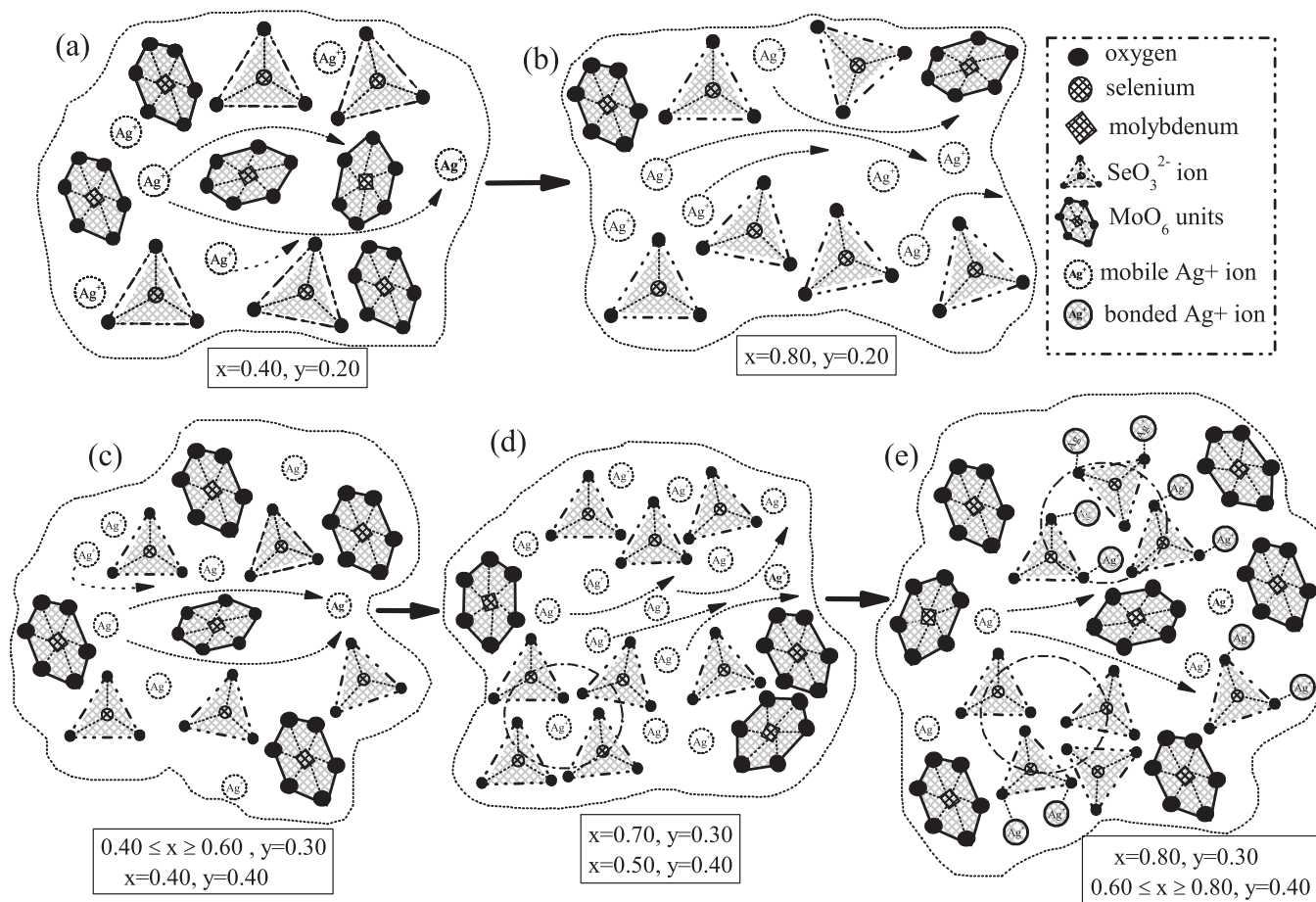


FIG. 7. Schematic 2D representation of the modification of glass network structure depending on modifier and formers ratio for the glasses of compositions $y\text{Ag}_2\text{O}-(1-y)(x\text{SeO}_2-(1-x)\text{MoO}_3)$: (a) for $x=0.40$, $y=0.20$; (b) for $x=0.80$, $y=0.20$; (c) for $x=0.40$, $y=0.30$ and $x=0.40$, $y=0.40$; (d) for $0.50 \leq x \leq 0.70$, $y=0.30$ and $x=0.50$, $y=0.40$; (e) $x=0.80$, $y=0.30$ and $0.60 \leq x \leq 0.80$, $y=0.40$. The arrow between (a) and (b) indicates the structural modification and transition stages for $x > 0.40$. The arrow between (c) and (d) indicates the structural modification and transition stages as $x > 0.40$ for the $y=0.30$ series. Similarly the arrow between (d) and (e) indicates the structural modification occurring for $x > 0.50$ for the $y=0.40$ series. The curved arrows in the figures indicate conduction pathways.

also mobile ion concentration increases to some extent thus enhancing the conductivity. Fig. 7(e) represents the structure for $y=0.30$, $x=0.80$ composition where a small decrease in the available free volume occurs due to increase of isolated crystalline silver selenite and molybdate units, and a decrease of mobile ion concentration also occurs, thus decreasing the conductivity effectively. Fig. 7(e) also represents the possible structures for the $y=0.40$, $x \geq 0.60$ compositions where there is a decrease in available free volume due to the increase of isolated crystalline silver selenite and molybdate units and decrease of mobile ion concentration, which in turn decreases the conductivity. The schematic diagram thus signifies the microscopic modification of the glass network structure with composition and thus correlates to the macroscopic ion transport properties.

IV. CONCLUSIONS

Ion transport in Ag^+ conducting selenomolybdate mixed former glasses has been studied by changing modifier as well glass formers ratio. The conductivity shows strong dependence on the modifier content as well as on the glass formers ratio. For the low modified glasses, the dc conductivity

increases gradually with increase of SeO_2 content. For highly modified glasses, the dc conductivity shows maxima depending on glass formers ratio. It is observed that the change in the ion-ion distance and dielectric constant causes the observed variation in the ionic conductivity or the activation energy. The characteristic length scales signifying the spatial extent of sub-diffusive ion dynamics and the transition from sub-diffusive to diffusive region show a strong dependency on the glass compositions. For low SeO_2 content, the vibration of SeO_3^{2-} ion dominates, whereas at higher SeO_2 content, the vibration of isolated MoO_6 units dominates. From the estimation of mobile ion concentration along with results obtained from FTIR spectroscopy, a schematic structural of the modification of glass network has been proposed, indicating dual role of SeO_2 . Here for low modified glasses at lower SeO_2 content, SeO_2 behaves as modifier which depolymerizes the glass network creating non-bridging oxygen which behaves like hopping sites, thereby increases the conductivity with increasing SeO_2 , whereas for highly modified glasses at higher SeO_2 content, SeO_2 acts as glass former which polymerizes the glass network, thereby lowering the effective hopping sites which in turn decreases the conductivity.

ACKNOWLEDGMENTS

Financial support for the work by the Department of Science and Technology, Government of India via Project No. SR/S2/CMP-0093/2010 (G) is thankfully acknowledged.

- ¹P. Knauth, *Solid State Ionics* **180**, 911 (2009).
²J. W. Fergus, *Sens. Actuators B* **134**, 1034 (2008).
³D. Dutta and A. Ghosh, *Phys. Rev. B* **72**, 024201 (2005).
⁴P. Mustarelli, L. Linati, V. Tartara, C. Tomasi, and A. Magistris, *Solid State Nucl. Magn. Reson.* **27**, 112 (2005).
⁵D. I. Novita, P. Boolchand, M. Malki, and M. Micoulaut, *Phys. Rev. Lett.* **98**, 195501 (2007).
⁶A. Dutta and A. Ghosh, *J. Non-Cryst. Solids* **351**, 203 (2005); M. Sural and A. Ghosh, *Solid State Ionics* **130**, 259 (2000).
⁷G. N. Greaves and S. Sen, *Adv. Phys.* **56**, 1 (2007).
⁸A. Sanson, F. Rocca, C. Armellini, G. Dalba, P. Fornasini, and R. Grisenti, *Phys. Rev. Lett.* **101**, 155901 (2008).
⁹K. Minami, A. Hayashi, and M. Tatsumisago, *Solid State Ionics* **181**, 1505 (2010).
¹⁰D. Coppo, M. J. Duclot, and J. L. Souquet, *Solid State Ionics* **90**, 111 (1996).
¹¹D. Zielniok, H. Eckert, and C. Cramer, *Phys. Rev. Lett.* **100**, 035901 (2008).
¹²Y. B. Dimitriev, S. I. Yordanov, and L. I. Lakov, *J. Non-Cryst. Solids* **192&193**, 179 (1995).
¹³C.-H. Lee, H.-J. Sohn, and M. G. Kim, *Solid State Ionics* **176**, 1237 (2005).
¹⁴M. Schuch, C. R. Muller, P. Maass, and S. W. Martin, *Phys. Rev. Lett.* **102**, 145902 (2009).
¹⁵J. C. Dyre, P. Maass, B. Roling, and D. L. Sidebottom, *Rep. Prog. Phys.* **72**, 046501 (2009).
¹⁶O. L. Anderson and D. A. Stuart, *J. Am. Ceram. Soc.* **37**, 573 (1954).
¹⁷T. Minami, *J. Non-Cryst. Solids* **73**, 273 (1985).
¹⁸K. Yonashiro and M. Iha, *J. Phys. Soc. Jpn.* **70**, 2958 (2001).
¹⁹P. Mustarelli, C. Tomasi, A. Magistris, and L. Linati, *Phys. Rev. B* **63**, 144203 (2001).
²⁰Y. Kim, J. Saienga, and S. W. Martin, *J. Phys. Chem. B* **110**, 16318 (2006).
²¹B. Deb and A. Ghosh, *J. Appl. Phys.* **112**, 024102 (2012).
²²D. L. Sidebottom, *Rev. Mod. Phys.* **81**, 999 (2009).
²³B. Roling, C. Martiny, and S. Bruckner, *Phys. Rev. B* **63**, 214203 (2001).
²⁴M. Micoulaut and M. Malki, *Phys. Rev. Lett.* **105**, 235504 (2010).